BACE overexpression alters the subcellular processing of APP and inhibits Aβ deposition in vivo

Edward B. Lee,[1] Bin Zhang,[1] Kangning Liu,[1] Eric A. Greenbaum,[1] Robert W. Doms,[2] John Q. Trojanowski,[1,3] and Virginia M.-Y. Lee[1,3]

[1]The Center for Neurodegenerative Disease Research, Department of Pathology and Laboratory Medicine, [2]Department of Microbiology, and [3]Institute on Aging, University of Pennsylvania School of Medicine, Philadelphia, PA 19104

Introducing mutations within the amyloid precursor protein (APP) that affect β- and γ-secretase cleavages results in amyloid plaque formation in vivo. However, the relationship between β-amyloid deposition and the subcellular site of Aβ production is unknown. To determine the effect of increasing β-secretase (BACE) activity on Aβ deposition, we generated transgenic mice overexpressing human BACE. Although modest overexpression enhanced amyloid deposition, high BACE overexpression inhibited amyloid formation despite increased β-cleavage of APP. However, high BACE expression shifted the subcellular location of APP cleavage to the neuronal perikarya early in the secretory pathway. These results suggest that the production, clearance, and aggregation of Aβ peptides are highly dependent on the specific neuronal subcellular domain wherein Aβ is generated and highlight the importance of perikaryal versus axonal APP proteolysis in the development of Aβ amyloid pathology in Alzheimer's disease.

Introduction

Although the characteristic lesions of Alzheimer's disease (AD), amyloid plaques and neurofibrillary tangles, have been recognized for almost a century, the mechanisms whereby these deposits accumulate in vivo are still largely unknown. Aβ peptides are the major constituent of amyloid plaques and are produced by sequential proteolysis of amyloid precursor protein (APP) by β- and γ-secretase (Wilson et al., 1999). Amyloid plaques are formed in vivo upon overexpressing APP mutations that shift γ-cleavage toward the production of the more amyloidogenic 42–amino acid variant of Aβ ($Aβ_{42}$; Games et al., 1995), or by direct manipulation of γ-secretase by introducing mutations within presenilin, a subunit of the multimeric γ-secretase complex (Borchelt et al., 1997). APP mutations that increase β-cleavage also result in Aβ deposition (Hsiao et al., 1996).

An aspartyl protease, BACE, is the major β-secretase (Sinha et al., 1999; Vassar et al., 1999; Yan et al., 1999; Lin et al., 2000). BACE cleaves either at Asp1 or Glu11 (numbering relative to the first amino acid in Aβ) to release NH_2-terminal ectodomains referred to as sAPPβ and sAPPβ′, respectively (Fig. 2 A). The remaining membrane-bound COOH-terminal APP fragments are then cleaved by γ-secretase to produce full-length $Aβ_{1\text{-}40/42}$ or the NH_2-terminally truncated $Aβ_{11\text{-}40/42}$. BACE overexpression in neuronal (E.B. Lee et al., 2003) and nonneuronal cells (Vassar et al., 1999; Huse et al., 2002; Liu et al., 2002) increases Aβ generation, whereas genetic ablation of BACE eliminates Aβ production (Cai et al., 2001; Luo et al., 2001).

Less is known about the significance of the subcellular localization of APP processing with respect to amyloid plaque formation. In addition to the ER and the Golgi apparatus, APP is enriched in axons and presynaptic terminals (Schubert et al., 1991; Ferreira et al., 1993). Although Aβ is generated in several different organelles in vitro (Wilson et al., 1999), the subcellular site of Aβ generation in vivo is more difficult to assess. However, studies indicate that APP undergoes kinesin I–dependent vesicular fast axonal transport (Koo et al., 1990; Ferreira et al., 1993) and that APP proteolysis may occur within axonal or presynaptic vesicles (Buxbaum et al., 1998). Furthermore, synaptic activity increases Aβ secretion, indicating that the presynaptic terminal is an important regulatory site for Aβ generation (Kamenetz et al., 2003). Finally, ablation of the perforant pathway in APP transgenic (Tg) mice decreases amyloid plaque deposition in the hippocampus, suggesting that synaptic Aβ contributes to plaque formation (Lazarov et al., 2002; Sheng et al., 2002).

Correspondence to Virginia M.-Y. Lee: vmylee@mail.med.upenn.edu

Abbreviations used in this paper: AD, Alzheimer's disease; APP, amyloid precursor protein; BACE, β-secretase; FA, formic acid; IDE, insulin-degrading enzyme; NFM, molecular weight neurofilament subunit; PhAT, anti–phospho-APP-threonine 668; PrP, prion protein; Tg, transgenic.

The online version of this article contains supplemental material.

The Journal of Cell Biology, Vol. 168, No. 2, January 17, 2005 291–302
http://www.jcb.org/cgi/doi/10.1083/jcb.200407070

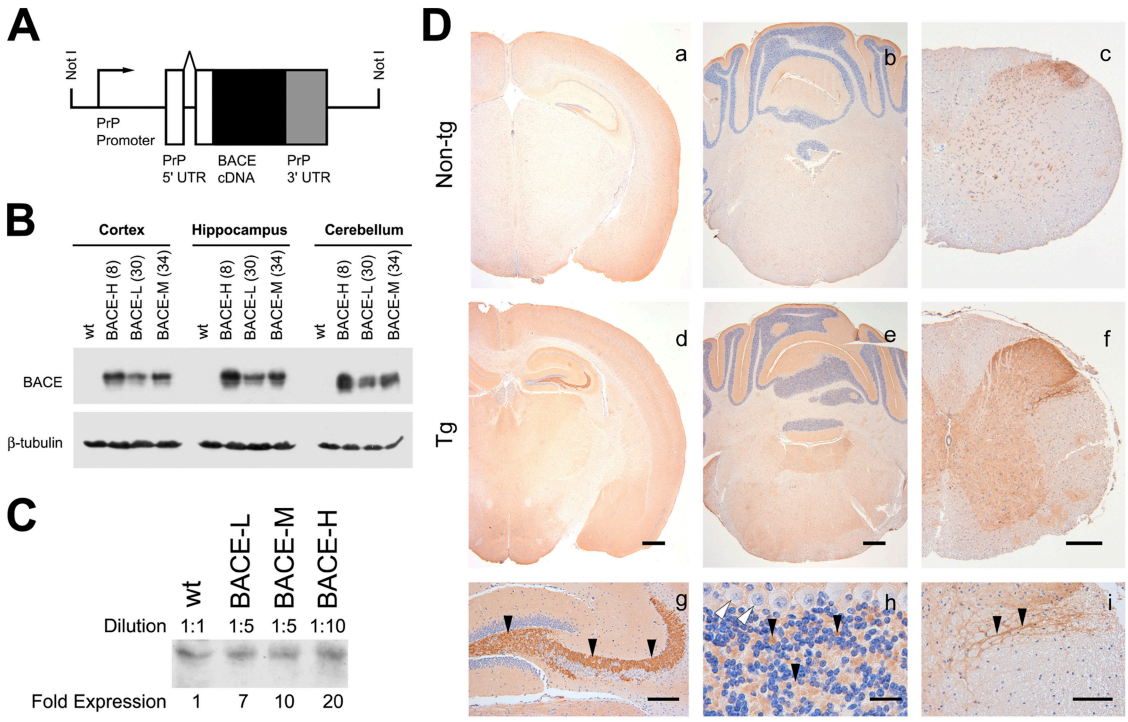

Figure 1. **Generation of Tg mice overexpressing human BACE.** (A) Schematic of the expression cassette used to generate PrP-BACE mice, containing the human BACE cDNA flanked by the 5′ UTR of the murine PrP gene containing an intron, and the 3′ UTR of the PrP gene. (B) BACE expression in Tg mice. RIPA lysates from the cortex, hippocampus, and cerebellum were immunoblotted for BACE using an antibody against the COOH terminus of human BACE. Three Tg lines ($n > 3$; shown are mice at 14–16 mo) were analyzed with low (30), medium (34), and high (8) expression. (C) BACE expression relative to non-Tg mice. Cortical RIPA lysates were diluted as indicated before immunoblotting for BACE using a polyclonal antisera against the entire NH_2-terminal ectodomain of BACE. BACE-L, -M, and -H mice overexpress ~7-, 10-, and 20-fold more BACE than non-Tg mice ($n > 3$ per genotype). No age-dependent changes in BACE expression have been observed (up to 20 mo). (D) Regional expression of BACE. Immunohistochemistry using BACE-N1 demonstrates increased immunoreactivity in BACE overexpressing mice. Representative images are shown of the cortex, striatum, cerebellum, brainstem, and spinal cord. Higher magnification shows staining of mossy fiber terminals, the granule cell layer of the cerebellum, and the dorsal spinal cord. Sections from APP (a–c) and BACE-H (d–i) mice are shown. Black arrowheads demonstrate synaptic/axonal staining, whereas white arrowheads show Purkinje cells. Wild-type/APP or BACE/BACExAPP mice showed no differences in staining ($n > 2$ per genotype). Similar staining was observed with a polyclonal antibody raised against the COOH terminus of BACE and polyclonal antibodies raised against the ectodomain of BACE. Bars: (a and d) 500 μm; (b and e) 500 μm; (c and f) 250 μm; (g) 150 μm; (h) 25 μm; (i)100 μm.

A priori, increased BACE activity is expected to increase Aβ pathology. Indeed, modest BACE overexpression in mice increases steady-state Aβ levels (Bodendorf et al., 2002). However, we discovered that high BACE overexpression paradoxically decreased Aβ deposition despite enhanced β-cleavage of APP. Furthermore, we found that BACE overexpression altered the subcellular localization of BACE cleavage by increasing β-cleavage early in the secretory pathway, thereby depleting APP destined for axonal transport. These unexpected findings underscore the importance of the subcellular site of Aβ generation in the pathogenesis of AD.

Results

Generation of BACE Tg mice

To determine whether increased BACE activity affects Aβ deposition in vivo, we produced three lines of Tg mice expressing different levels of human BACE driven by the prion protein (PrP) promoter (Fig. 1 A), determined by immunoblotting of cortical, hippocampal, and cerebellar lysates (Fig. 1 B). Line 30 expressed the lowest amount of BACE, followed by lines 34 and 8 (hereafter named BACE-L, BACE-M, and BACE-H, respectively), expressing BACE ~7-, 10-, and 20-fold over endogenous levels (Fig. 1 C and Fig. 2 B). Increased BACE expression (Fig. 1 D) was also noted by immunohistochemistry which, in addition to neuronal cell bodies, demonstrated BACE staining in axons and synaptic elements such as the mossy fiber terminals of the hippocampus, puncta within the granule cell layer of the cerebellum, and neuropil within the spinal cord (Fig. 1 D, g–i), suggesting that BACE is subject to anterograde axonal transport.

APP processing in BACE Tg mice

To determine the effects of BACE expression on APP processing and Aβ production in vivo, we crossed BACE Tg lines with the tg2576 mouse model overexpressing APPswe (Hsiao et al., 1996), and APP processing in these bigenic mice was studied by following the fate of the APP fragments shown in Fig. 2 A. BACE expression was similar in single BACE and bigenic APPx-BACE mice (Fig. 2 B). However, BACE overexpression altered the banding pattern of total APP (i.e., full-length APP as well as secreted APP ectodomains), apparent for both exogenous (light exposure) and endogenous (dark exposure) APP. To better understand the effect of BACE expression on APP pro-

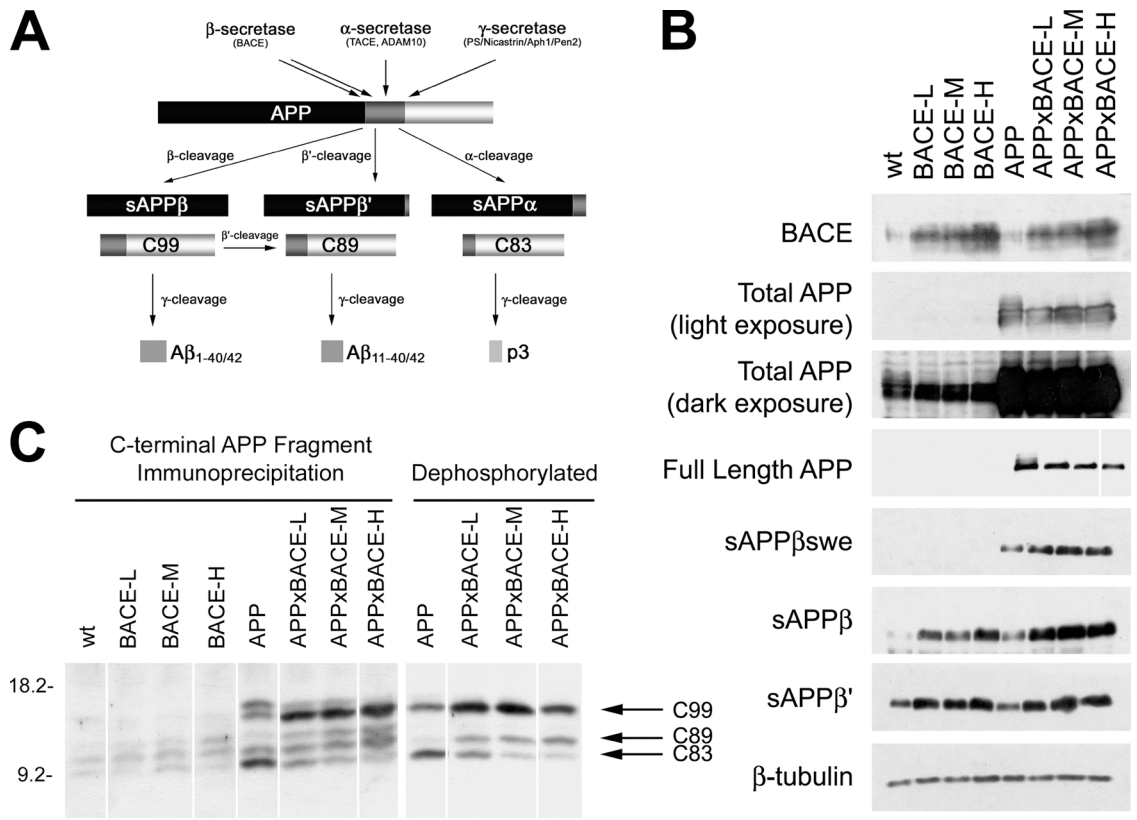

Figure 2. **Increase in β-cleavage due to BACE overexpression.** (A) Diagram of sequential APP processing by BACE, α-secretase, and γ-secretase. (B) Steady-state levels of BACE and APP in monogenic and bigenic mice. RIPA lysates from wild-type, BACE, APP, and APPxBACE Tg mice (n = 3–5 per genotype) were immunoblotted for BACE and several APP species. BACE was probed with 84 (anti-BACE ectodomain). Total APP including full-length APP and all sAPP species was probed with Karen (anti–NH_2 terminal APP). Two exposures are shown for optimal visualization of exogenous (light) and endogenous (dark) APP. Full-length APP was probed with 4G8. sAPPβswe, sAPPβ, and sAPPβ′ were probed with end-specific antibodies 54, C5A4 and C10A4, respectively. An immunoblot for β-tubulin is shown to demonstrate equal loading in all lanes. (C) Steady-state levels of COOH-terminal APP fragments in monogenic and bigenic mice. Whole brain RIPA lysates from wild-type, BACE, APP, and APPxBACE Tg mice were immunoprecipitated and immunoblotted with 5685 to recover COOH-terminal APP fragments. Select immunoprecipitates were dephosphorylated (right) before electrophoresis. White lines indicate that intervening lanes have been spliced out.

teolysis, immunoblots specific for different APP species were performed. Full-length APP, predominantly the *N*- and *O*-glycosylated forms of APP detected by 4G8 (anti-$A\beta_{17-24}$), was reduced by BACE overexpression, which is consistent with increased APP proteolysis. This decrease in full-length APP was paralleled by an increase in BACE-derived sAPP species (Fig. 2 B) including sAPPβswe (generated from exogenous APPswe), sAPPβ (generated from endogenous APP), and sAPPβ′ (produced by cleavage at the Glu11 cleavage site). Therefore, BACE overexpression resulted in increased β-cleavage of both exogenous and endogenous APP.

Increased BACE activity also altered steady-state levels of COOH-terminal APP fragments (Fig. 2 C). In monogenic BACE mice, BACE-derived COOH-terminal APP fragments, predominantly C89, were increased relative to wild-type mice, which is consistent with the preferential cleavage of rodent APP at position 11 within Aβ (Wang et al., 1996; Gouras et al., 1998; Cai et al., 2001). In APP overexpressing mice, five distinct bands corresponding to APP COOH-terminal fragments were apparent (Fig. 2 C). Several of these bands correspond to phosphorylated COOH-terminal APP fragments as dephosphorylation with alkaline phosphatase collapsed the five bands into three bands corresponding to C99, C89, and C83 (Fig. 2 C, left vs. right). As expected, BACE overexpression increased steady-state levels of C99 and C89, whereas α-secretase–derived C83 was decreased, which is consistent with a subcellular competition between α- and β-cleavage (Skovronsky et al., 2000). Interestingly, despite an overall increase in C99, BACE overexpression decreased the amount of phospho-C99 by ~50–60% in APPxBACE-L and APPxBACE-M mice and over 80% in APPxBACE-H mice.

Decreased steady-state Aβ due to BACE overexpression

We hypothesized that the increase in C99 would be paralleled by an increase in Aβ. Surprisingly, ELISA quantification of steady-state Aβ from young mice (5–7 mo) indicated that high BACE expression paradoxically decreased full-length Aβ production (Fig. 3 A). Although very high BACE overexpression in cell culture models results in cleavage at positions 11 and 34 within Aβ, immunoprecipitation of brain lysates with 4G8, albeit less quantitative than ELISA methods, failed to detect any peptides other than full-length Aβ and p3 (Fig. 3 B). Thus, truncated Aβ peptides such as $A\beta_{1-34}$ and $A\beta_{11-40/42}$ are pro-

duced at very low levels relative to full-length Aβ, or are rapidly degraded in vivo. To confirm the lack of NH_2-terminally truncated Aβ peptides, additional ELISA's were performed to detect either full-length $Aβ_{1-40/42}$ or total $Aβ_{x-40/42}$ (Fig. 3, C and D). Equivalent amounts of $Aβ_{1-40/42}$ and $Aβ_{x-40/42}$ were detected suggesting that NH_2-terminally truncated Aβ species were present at very low levels. These results were corroborated by the near absence of truncated Aβ in amyloid deposits of older Tg mice (Fig. S1, available at http://www.jcb.org/cgi/content/full/jcb.200407070/DC1).

Decreased Aβ deposition due to BACE overexpression

Monogenic BACE mice showed no evidence of Aβ deposition (unpublished data). Therefore, to determine the impact of BACE overexpression on Aβ deposition, we evaluated APP and APPxBACE mice at 14–16 mo old for amyloid plaque pathology. As shown by thioflavin S staining, APPxBACE-L mice exhibited increased amyloid plaque formation within the cortex (Fig. 4 A). However, higher levels of BACE expression dramatically decreased thioflavin S positive cortical deposition of Aβ amyloid. Essentially identical results were obtained by performing immunohistochemistry using NAB228 (anti-$Aβ_{1-11}$) or 4G8 (anti-$Aβ_{17-24}$), indicating that the observed decrease was not due to a shift from fibrillar to diffuse Aβ deposits. Unlike cortical amyloid plaques, hippocampal Aβ deposits were diminished even in the BACE-L mice, whereas the BACE-M and BACE-H lines showed virtually no hippocampal Aβ deposits. Quantification of amyloid burden showed that APPxBACE-L mice displayed a significantly higher amyloid burden within the somatosensory cortex with a corresponding decrease in amyloid burden in the hippocampus (Fig. 4, B–D). Higher BACE expression inhibited Aβ deposition within both the cortex and the hippocampus.

We confirmed our morphological results by quantitative Aβ ELISA after sequential extraction of brain regions with RIPA buffer followed by formic acid (FA) to obtain detergent soluble and insoluble fractions. Consistent with the histological results, cortical Aβ was slightly higher in APPxBACE-L mice in both soluble and insoluble fractions when compared with monogenic APP mice (Fig. 5, A and B), whereas higher BACE expression inhibited cortical Aβ accumulation. BACE overexpression also decreased hippocampal Aβ levels in both soluble and insoluble fractions for all three BACE overexpressing lines (Fig. 5, C and D). Aβ levels were very low in the cerebellum, which is consistent with the lack of cerebellar amyloid plaques (Fig. 5, E and F). Thus, although a modest increase in BACE activity, especially in the neocortex, enhanced the deposition of Aβ, larger increases in BACE activity had the unexpected, opposite result.

Biochemical markers of APP maturation in APPxBACE axons

Two findings pointed to diminished axonal transport of APP as the cause for the unexpected discrepancy between increased C99 and decreased Aβ. First, the dissociation between cortical and hippocampal amyloid in APPxBACE-L mice suggested that BACE overexpression altered Aβ deposition via a mechanism related to the spatial location of APP processing. Second, phospho-C99 is the only BACE-derived APP species that was decreased in a dose-dependent manner upon BACE overexpression (Fig. 2 C and Fig. 6 A). This suggested that phospho-C99 may be the precursor to Aβ peptides that eventually de-

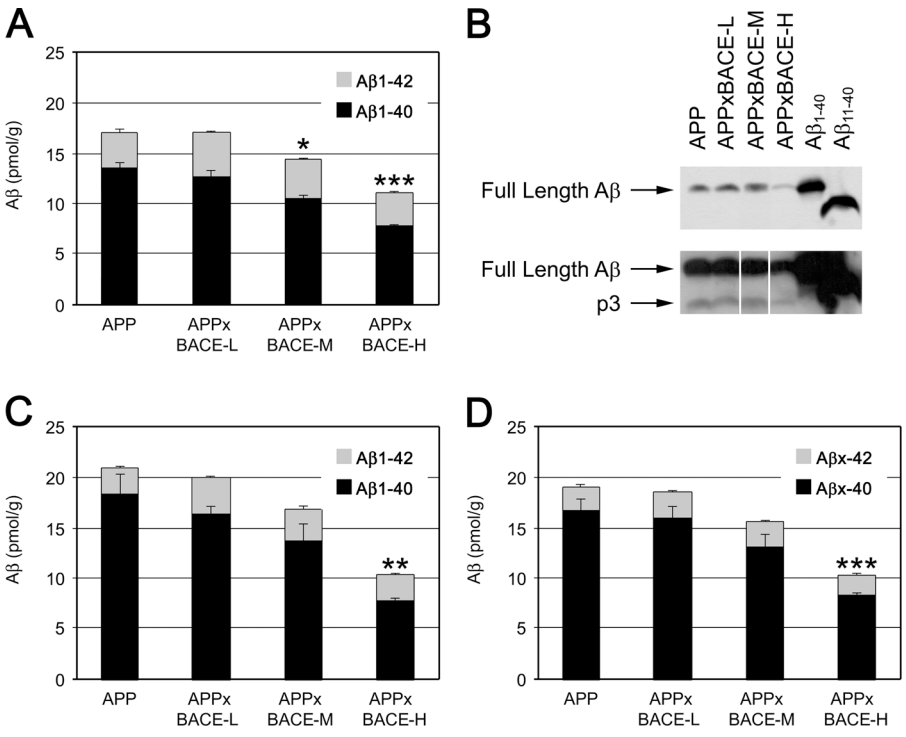

Figure 3. **BACE overexpression decreases steady-state Aβ levels.** (A) Dose-dependent decrease in steady-state Aβ. Steady-state Aβ levels from RIPA cortical lysates (APP, $n = 5$; APPxBACE, $n = 3$ per genotype, 5–7 mo old) were quantified by Ban50-BA27/BC05 sandwich ELISA for full-length $Aβ_{40}$ and $Aβ_{42}$. (ANOVA, $P < 0.0001$; Bonferroni's post-hoc relative to APP, $^*P < 0.05$, $^{***}P < 0.001$). (B) RIPA lysates were subject to immunoprecipitation with 4G8, followed by electrophoresis on a 10/16.5% Tris-tricine gel. Immunoblotting with 4G8 demonstrates the presence of full-length Aβ and p3 with little NH_2- or COOH-terminally truncated Aβ variants ($n = 2$ per genotype). An overexposure of the immunoblot is shown to demonstrate the presence of p3 and the absence of other truncated Aβ peptides. White lines indicate that intervening lanes have been spliced out. (C) Steady-state Aβ levels from RIPA cortical lysates ($n = 3$–5 mice per genotype, 5–7 mo old) were quantified by JRF/c40-AβN or JRF/c42-AβN ELISA for full-length $Aβ_{40}$ and $Aβ_{42}$. (ANOVA, $P = 0.0019$; Bonferroni's post-hoc relative to APP, $^{**}P < 0.01$). (D) Steady-state Aβ levels from RIPA cortical lysates ($n = 3$–5 mice per genotype, 5–7 mo old) were quantified by JRF/c40-m266 or JRF/c42-m266 ELISA for total (full-length and NH_2-terminally truncated) $Aβ_{40}$ and $Aβ_{42}$. (ANOVA, $P = 0.0015$; Bonferroni's post-hoc relative to APP, $^{***}P < 0.001$).

posit into amyloid plaques, which is consistent with an increase in phospho-C99 in AD brains (M.S. Lee et al., 2003). The localization of phospho-APP in post-Golgi vesicles within dendrites and axons (Ando et al., 1999; Iijima et al., 2000; M.S. Lee et al., 2003) suggests that APP phosphorylation occurs late in the secretory pathway. Therefore, we hypothesized that enhanced BACE expression leads to increased APP cleavage early in the secretory pathway, depleting APP before its transport to the presynaptic terminal.

If BACE cleavage occurs early in the secretory pathway, markers of APP maturation should be reduced in APPxBACE mice. Indeed, *N*- and *O*-glycosylated APP and phospho-C99 were both reduced upon BACE overexpression (Fig. 2). To better assess the levels of phospho-APP, we generated an anti–phospho-APP-threonine 668 (PhAT), phosphorylation-specific antibody. Although antisera 5685 immunoprecipitated both nonphosphorylated and phosphorylated C99, PhAT recognized only the slower migrating phospho-C99 (Fig. 6 A). As predicted, we observed a marked decrease in phospho-Thr668-C99 in cortical extracts derived from APPxBACE mice. Furthermore, phospho-APP was recovered from monogenic APP mice but not bigenic APPxBACE mice (Fig. 6 A). We also found that only fully glycosylated APP is phosphorylated at Thr668 corroborating reports that APP phosphorylation occurs late in the secretory pathway after acquisition of *O*-linked carbohydrates within the Golgi (Ando et al., 1999; Iijima et al., 2000). Moreover, mature, phospho-APP was decreased in every brain region analyzed in APPxBACE-H mice including the corpus callosum and sciatic nerve (Fig. 6 B). This absence of phospho-APP upon BACE overexpression suggests that APP within post-Golgi compartments is greatly reduced.

To demonstrate that phospho-APP is selectively transported by fast anterograde axonal transport and that this pool of APP is diminished upon BACE overexpression, we radiolabeled retinal ganglion cells by intravitreal injections of [^{32}P]PO_4 (Fig. 6 C) followed by immunoprecipitation of optic nerve lysates for full-length APP. Radiolabeled phospho-APP was present within optic nerves of APP Tg mice, whereas no radiolabeled APP was

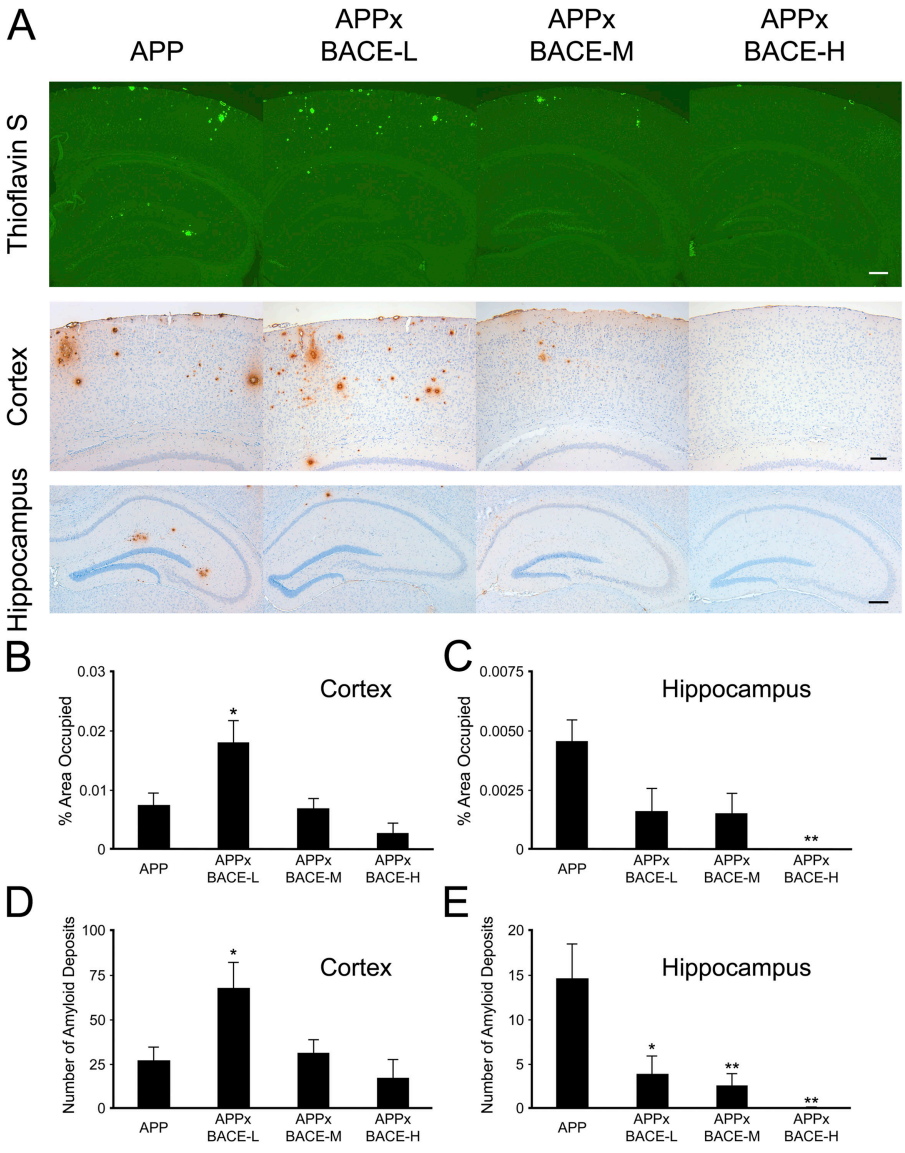

Figure 4. **BACE overexpression inhibits Aβ amyloid formation.** (A) Sections from APP or APPxBACE (-L, -M, and -H) littermates ($n > 4$ mice per genotype) were stained with thioflavin S for fibrillar amyloid deposits. Sections are from 14-mo-old mice, except for sections from APPxBACE-H mice which are 16 mo old. To corroborate thioflavin S staining, sections from the cortex and hippocampus were stained with NAB228. Bars: (top) 200 μm; (middle) 100 μm; (bottom) 200 μm. (B–D) Amyloid burden from sections (four sections/mouse) of APP or APPxBACE (-L, -M, and -H) littermates stained with NAB228 were analyzed by quantitative image analysis ($n = 4$ mice/genotype). For the somatosensory cortex, the percent area occupied by Aβ deposits (B, ANOVA, $P = 0.05$) and the number of Aβ deposits per section (C, ANOVA, $P = 0.0219$) are increased in APPxBACE-L mice relative to APP mice (Bonferroni's post-hoc relative to APP, $^*P < 0.05$), whereas further increases in BACE expression inhibited Aβ deposition. For the hippocampus, the percent area occupied by Aβ deposits (C, ANOVA, $P = 0.0099$) and the number of Aβ deposits per section (D, ANOVA, $P = 0.0034$) indicated that BACE expression decreased Aβ deposition in all three BACE overexpressing lines. (Bonferroni's post-hoc relative to APP, $^*P < 0.05$, $^{**}P < 0.01$).

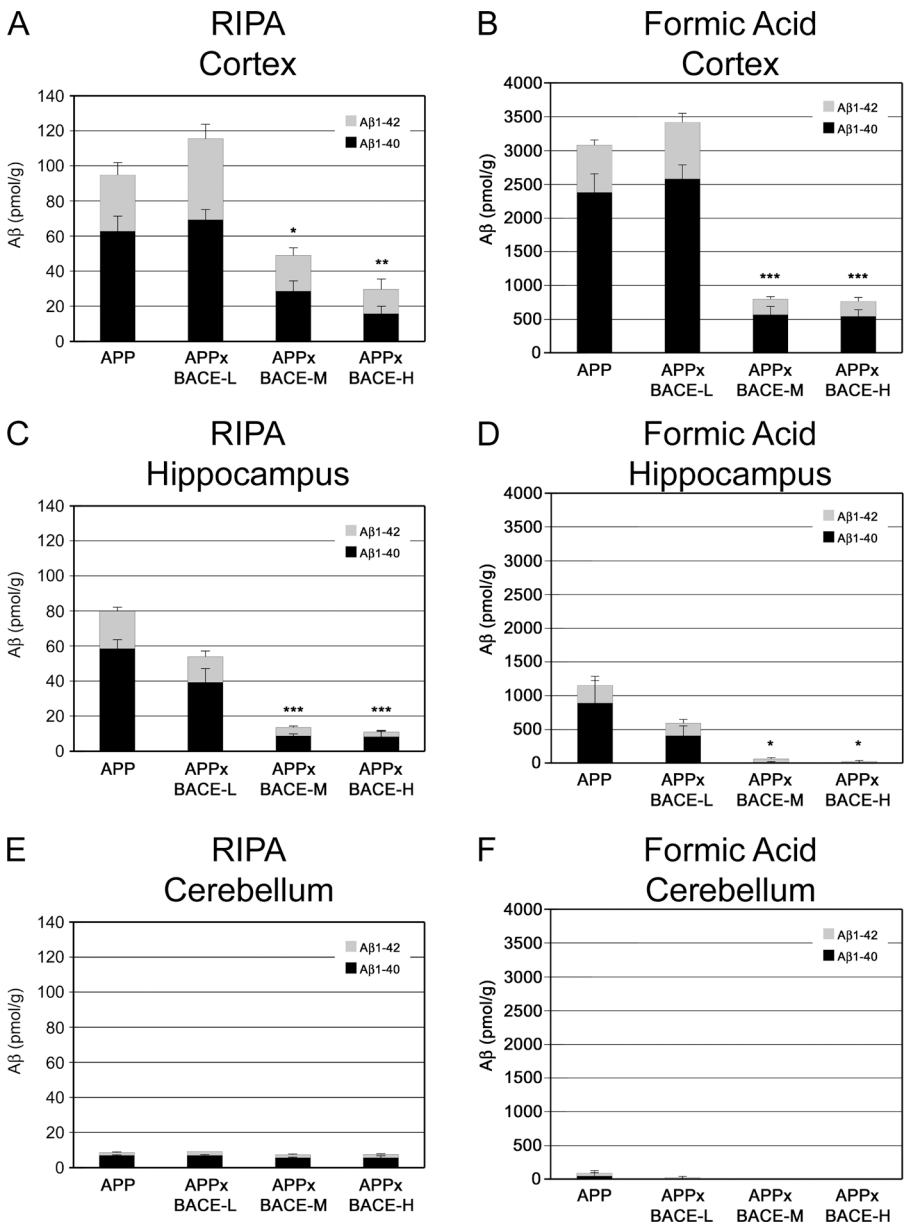

Figure 5. **Quantification of Aβ accumulation in APP and APPxBACE mice.** Different brain regions were sequentially extracted in RIPA buffer and 70% FA to obtain detergent-soluble and insoluble fractions. Aβ was quantified by Ban50-BA27/BC05 sandwich ELISA for full-length $A\beta_{40}$ and $A\beta_{42}$. All mice were 14 mo old except APPxBACE-H mice, which were 16 mo old. Quantification of soluble and insoluble cortical Aβ (A and B) indicated that relative to APP mice ($n = 3$ females, 1 male), low BACE expression (APPxBACE-L, $n = 3$ females, 1 male) increased cortical Aβ accumulation, whereas higher BACE expression inhibited Aβ accumulation (APPxBACE-M, $n = 2$ females, 1 male, and APPxBACE-H, $n = 2$ females, 1 male). ANOVA yielded $P = 0.0006$ and $P < 0.0001$ for soluble and insoluble cortical Aβ measurements, respectively. Quantification of soluble and insoluble hippocampal Aβ indicated that hippocampal Aβ accumulation decreased in a dose-dependent manner due to BACE overexpression (C and D). ANOVA yielded $P = 0.0002$ and 0.002 for soluble and insoluble hippocampal Aβ measurements, respectively. Both soluble and insoluble Aβ from the cerebellum were low in all genotypes (E and F). ANOVA failed to show any significance for data from cerebellar Aβ measurements. For cortical and hippocampal Aβ measurements, Bonferroni's post-test revealed significant differences relative to APP mice ($*P < 0.05$, $**P < 0.01$, $***P < 0.001$).

detected in optic nerves of APPxBACE-H mice (Fig. 6 D). Immunoblotting of the same nitrocellulose membrane showed that only fully glycosylated APP is phosphorylated, and that BACE overexpression selectively reduced mature APP within the optic nerve. Furthermore, the reduction in phospho-APP was specific because ^{32}P-labeled middle molecular weight neurofilament subunit (NFM) levels were not changed by BACE overexpression.

Decreased APP transport in APPxBACE mice

To further demonstrate that BACE overexpression resulted in a shift in the subcellular site of β-cleavage, axonal transport within sciatic nerves of APP or APPxBACE-H mice was interrupted by ligation for 6 h (Fig. 7 A), after which segments of the sciatic nerve proximal and distal to the ligature were assessed by immunoblotting for full-length APP, phospho-APP, and sAPPβswe. In monogenic APP mice, mature fully glycosylated APP isoforms proximal to the ligature were ~50% higher than in unligated sciatic nerves, whereas mature APP distal to the ligature was reduced by ~60%, confirming that mature APP is subject to fast axonal transport (Fig. 7 B). Immature APP levels were unchanged after nerve ligation, suggesting that this signal is not derived from axonally transported APP, which is consistent with reports showing that the PrP promoter drives expression within Schwann cells of the sciatic nerve (Follet et al., 2002). In APPxBACE-H mice, mature APP levels at steady-state in unligated sciatic nerves were over fourfold lower relative to monogenic APP mice. Furthermore, sciatic nerve ligation in APPxBACE-H mice resulted in only a slight accumulation of mature APP. Similar results were obtained when phospho-APP was immunoprecipitated by the PhAT antibody. Thus, BACE overexpression selectively decreases the anterograde axonal transport of mature phosphorylated isoforms of APP. Finally, to assess the amount of β-cleavage within the axonal compartment, we measured

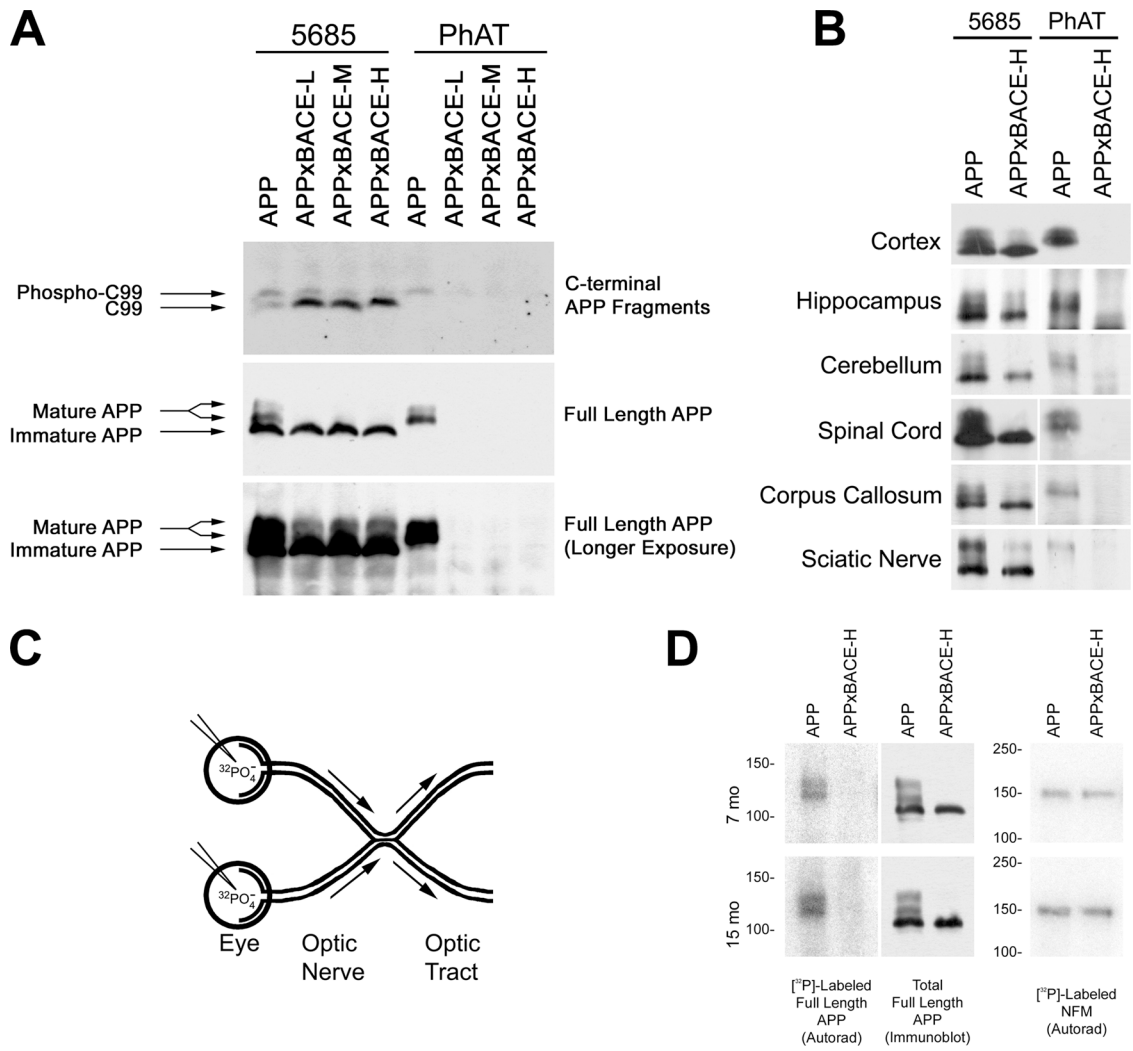

Figure 6. **Decreased mature, phospho-APP in APPxBACE axons.** (A) Biochemical markers of APP trafficking in APP and APPxBACE mice. Cortical lysates (n = 2–5 per genotype) were immunoprecipitated with 5685 (phosphorylation-independent COOH-terminal APP antibody) or PhAT and probed with NAB228 (anti-A$\beta_{1\text{-}11}$, top) for C99 or with Karen (anti–NH_2 terminus APP, bottom) for full-length APP. PhAT immunoprecipitations for full-length phospho-APP were performed with 10 times the material relative to 5685 immunoprecipitations. An overexposure of the immunoblot for full-length APP is shown to demonstrate the lack of immature APP in PhAT immunoprecipitates from APP mice, and the lack of phospho-APP in APPxBACE mice. (B) Regional analysis of mature APP species. RIPA lysates from various regions from APP or APPxBACE-H mice ($n > 2$ mice per genotype per region) were subject to immunoprecipitation with 5685 or PhAT followed by immunoblotting for full-length APP with Karen. White lines indicate that intervening lanes have been spliced out. (C) Intravitreal injections of ^{32}P-labeled orthophosphate label retinal ganglion cells which send axonal projections via the optic nerve. ^{32}P-labeled APP within the optic nerve is a measure of APP which has been phosphorylated and subject to anterograde axonal transport. (D) Transport of phospho-APP in optic nerves. 6 h after intravitreal injection of [^{32}P]PO_4, ^{32}P-labeled full-length APP was recovered by immunoprecipitation with 5685 from optic nerves from APP mice, but not APPxBACE-H mice (7 and 15 mo old). Immunoblot of the same nitrocellulose membrane shows that ^{32}P-labeled APP comigrates with only *N*- and *O*-glycosylated forms of APP, and that mature APP isoforms are depleted in optic nerves of APPxBACE-H mice. ^{32}P-labeled NFM levels, assessed by immunoprecipitation with RMO26, were not affected by BACE overexpression. Three pairs of mice were analyzed and showed similar results.

sAPPβswe levels proximal to the ligature in sciatic nerves of APP mice. The decrease in sAPPβswe produced within the proximal segment of the sciatic nerve in APPxBACE-H mice relative to APP mice (Fig. 7 B), coupled with the increase in sAPPβswe in total cortical lysates upon BACE overexpression (Fig. 2 A) indicates that APP cleavage had shifted from an axonal/synaptic compartment to the cell body.

Overexpression of both APP and BACE could potentially result in aberrant trafficking of either protein. To rule out artifacts induced by APP overexpression, sciatic nerve ligations were performed in non-Tg and monogenic BACE mice (Fig. 7 C). Again, mature forms of endogenous APP accumulated proximal to the ligature in non-Tg mice, and the amount of mature APP accumulation was greatly reduced upon BACE overexpression. Furthermore, to exclude the possibility that BACE overexpression nonspecifically affects axonal transport in general, a panel of proteins subject to fast and slow, anterograde and retrograde transport were assessed. No differences under steady-state conditions or upon ligation were noted in non-Tg or BACE Tg mice for kinesin, synaptophysin, dynein, neurofilament or β-tubulin. Therefore, the reduction in APP axonal transport cannot be attributed to aberrant localization of the overexpressed APP or to a nonspecific down-regulation of axonal transport upon BACE overexpression.

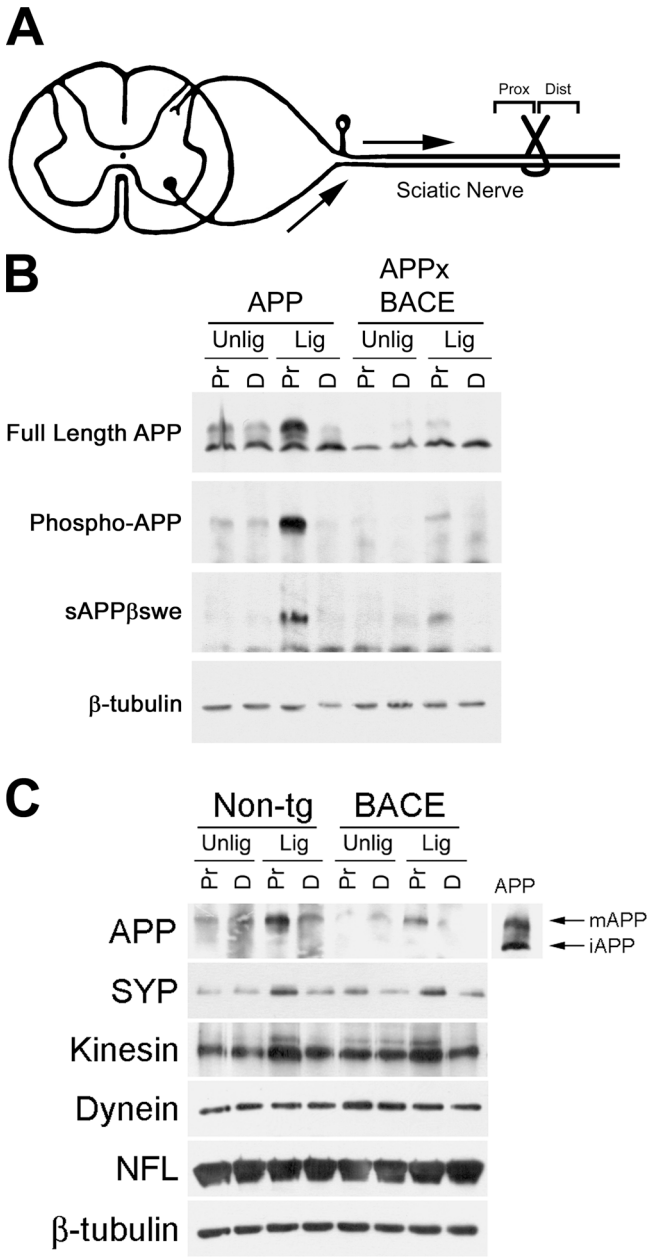

Figure 7. **Decreased axonal transport and processing of APP in APPxBACE mice.** (A) The sciatic nerve is a bundle of axons from sensory and motor neurons present in the dorsal root ganglion or the spinal cord. Upon ligation, proteins subject to anterograde axonal transport accumulate in the nerve segment proximal to the ligature. (B) Transport and processing of APP in ligated sciatic nerves. Sciatic nerves of APP or APPxBACE-H mice were ligated for 6 h. 5-mm segments proximal and distal to the ligature were homogenized, corrected for protein concentration, and immunoprecipitated with 5685 or PhAT. Segments from the unligated contralateral sciatic nerve were processed in parallel. Immunoprecipitates were immunoblotted with Karen for total full-length APP or full-length phospho-APP. Lysates were subject to another round of immunoprecipitation with Karen, followed by immunoblotting with 54 for sAPPβswe. Because β-tubulin levels are unchanged after 6 h of ligation, an immunoblot for β-tubulin is shown to demonstrate equal loading. Four pairs of mice were analyzed and showed similar results. (C) Endogenous APP axonal transport upon BACE overexpression. Sciatic nerves of non-Tg and monogenic BACE mice were ligated for 6 h (n = 3 pairs). Segments proximal and distal to the ligature were assessed for full-length APP by immunoprecipitation with 5685 and immunoblotting with Karen. Lysates were pooled due to the low level of endogenous APP within the sciatic nerve. Sciatic nerve from an APP mouse was run in parallel as a molecular weight marker. Immunoblots for synaptophysin, kinesin, dynein, NFL, and β-tubulin were also performed.

APP turnover and transport in Tg mice

To directly measure APP turnover in neuronal perikarya of BACE mice, pulse-labeling studies were performed in spinal cords and sciatic nerves. L5 spinal cord segments were injected with [^{35}S]-methionine to label newly synthesized APP within cell bodies of the spinal cord. After 30 min, no differences were found in radiolabeled full-length APP in spinal cords of non-Tg and BACE Tg mice indicating that APP synthesis is unaltered by BACE overexpression (Fig. 8, A and B). However, by 8 h, APP levels were significantly reduced in APPxBACE mice indicating that increased BACE activity hastens APP turnover. Significantly, *N*- and *O*-glycosylated APP was conspicuously reduced in BACE mice when compared with non-Tg mice at this time point. Furthermore, virtually no radiolabeled APP was recovered from sciatic nerves of BACE Tg mice, indicating once again that the rapid turnover of APP within neuronal cell bodies of the spinal cord results in a diminution in axonal transport of APP (Fig. 8, A and C).

Discussion

Both the amount and type of Aβ produced are important for AD pathogenesis. Thus, increased production of Aβ or increased production of Aβ1-42 relative to Aβ1-40 can accelerate the production of senile plaques and the development of AD. In addition, the subcellular sites where Aβ is produced may also play a role in AD pathogenesis. APP and the enzymes that cleave it colocalize throughout the secretory pathway, and Aβ can be produced at multiple intracellular sites. In neurons, APP undergoes fast anterograde transport to nerve terminals (Koo et al., 1990; Ferreira et al., 1993; Buxbaum et al., 1998), and is metabolized into Aβ peptides that are released and deposited as amyloid plaques around nerve terminals (Lazarov et al., 2002; Sheng et al., 2002). Thus, the axonal/synaptic fractions of APP appear particularly important in the generation of Aβ species that are ultimately deposited in amyloid plaques.

To further explore the relationships between the quantitative, qualitative and spatial factors that influence Aβ production and deposition, we produced Tg mice that expressed increased levels of BACE. Surprisingly, an inverse relationship between BACE expression and Aβ production/deposition was found. Our efforts to understand this paradoxical result led us to discover that BACE overexpression shifted the sites of APP processing such that APP proteolysis occurred predominantly in neuronal perikarya rather than in axons and axon terminals (Fig. 9). This alteration of APP processing upon BACE overexpression, together with the reduction of Aβ accumulation, indicates that Aβ generated proximally in neuronal perikarya has a different fate than Aβ that is generated at or near the synapse.

Several lines of evidence were provided to demonstrate the depletion of APP before axonal transport. First, BACE overexpression reduced α-cleavage as seen by the reduction in C83. Since our previous studies have shown that α-secretase competes with BACE within the TGN (Skovronsky et al., 2000), the reduction of C83 in APPxBACE mice suggests that β-cleavage of APP is enhanced within the TGN. Second, *N*- and *O*-glycosylated APP was reduced in BACE overexpressing

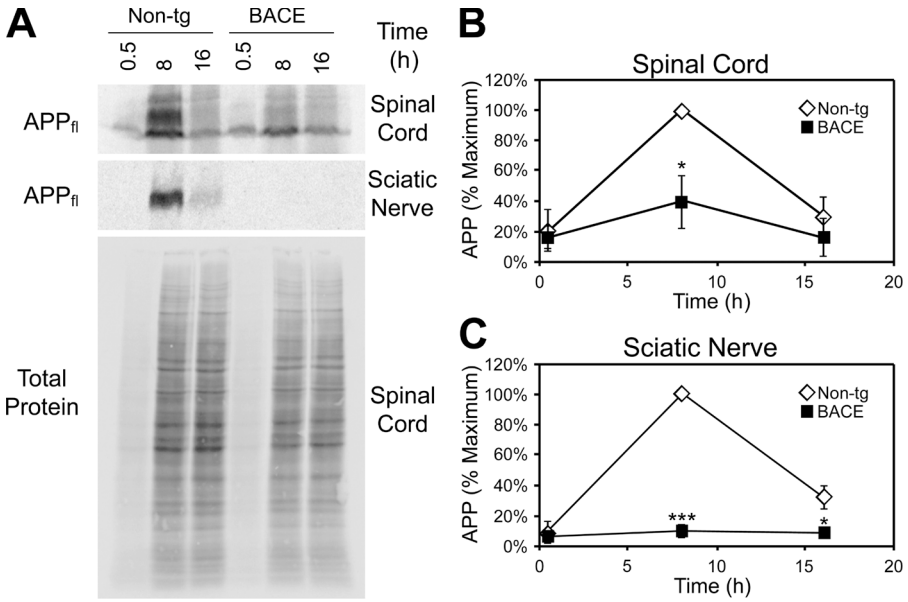

Figure 8. **Kinetic APP analysis of the spinal cord and sciatic nerve.** L5 segments of non-Tg and BACE Tg spinal cords were injected with [^{35}S]-methionine and analyzed at 0.5, 8, and 16 h after injection. (A) Full-length APP from spinal cords and sciatic nerves was immunoprecipitated with 5685 and electrophoresed on 7.5% Tris-glycine gels to examine the turnover of APP in vivo. Despite differences in APP levels, general radiolabeling of proteins is similar between non-Tg and BACE Tg mice, as determined by electrophoresis and autoradiography of immunoprecipitation supernatants. (B and C) Quantification of radiolabeled APP in spinal cords and sciatic nerves ($n = 3$ non-Tg, 2 BACE-H and 1 BACE-M per time point) demonstrated significantly lower levels of APP in both spinal cords and sciatic nerves (*$P < 0.05$, ***$P < 0.0001$), indicating that increased perikaryal APP proteolysis depletes mature, axonally transported APP.

mice indicating that APP is cleaved soon after carbohydrate processing in the Golgi apparatus. Third, although BACE overexpression increased C99 levels, the majority of C99 was not phosphorylated. In contrast, at least 50% of C99 was phosphorylated in monogenic APP mice. Because phosphorylation of threonine 668 of APP is a posttranslational modification found selectively within neuronal growth cones and neurites (Ando et al., 1999; Iijima et al., 2000), the lack of phospho-C99 indicates that APP cleavage in APPxBACE mice occurs in early compartments. Fourth, although mature full-length phospho-APP was readily detected from the corpus callosum, sciatic nerves and optic nerves of APP mice, almost no mature, phospho-APP was detected in APPxBACE bigenic mice demonstrating that APP was present only at very low levels in axons. Fifth, ^{32}P-labeled APP was dramatically reduced in optic nerves upon BACE overexpression, indicating that β-cleavage occurs before the phosphorylation and anterograde axonal transport of APP. Sixth, the reduction of APP accumulation upon sciatic nerve ligation supports the hypothesis that little intact APP is transported into axons in APPxBACE mice. Finally, pulse-labeling of spinal cords demonstrated that BACE overexpression increases APP turnover such that APP is not available for axonal transport. Notably, BACE overexpression did not alter APP synthesis, nor levels of immature ER-resident APP suggesting that APP cleavage is occurring within the Golgi after transit from the ER. Based on the evidence presented above, we concluded that BACE overexpression increases β-cleavage in proximal subcellular compartments, most likely within the Golgi apparatus, at the expense of axonal and synaptic APP (Fig. 9).

Despite increased β-cleavage, as evidenced by increased sAPPβ, sAPPβ′, sAPPβswe, and C99 levels in APPxBACE mice, Aβ levels were reduced by high BACE expression. This finding is contrary to cell culture models in which BACE overexpression leads to increased secretion of Aβ (Liu et al., 2002; E.B. Lee et al., 2003). One potential explanation of our results is that the fate of Aβ produced in neuronal perikarya and axonal terminals in the in vivo brain are different. For example, the microenvironment wherein Aβ is secreted may influence Aβ deposition. Synaptic zinc has been shown to play a role in Aβ aggregation and deposition, and depletion of synaptic zinc inhibits amyloid formation in vivo (Lee et al., 2002) suggesting that the environment within synaptic vesicles or the microenvironment at synaptic terminals is crucial to Aβ amyloidogenesis.

Alternatively, the differential fates of Aβ may be related to the localization of Aβ degrading activities in brain. Neprilysin is found predominantly in synapses and axons of smaller interneurons (Fukami et al., 2002). The localization and enzymatic properties of neprilysin are consistent with Aβ degrading activity within secretory vesicles and the plasma membrane (Iwata et al., 2000). In contrast, endothelin-converting enzyme is likely to degrade intracellular Aβ within acidic organelles such as the TGN (Schweizer et al., 1997; Eckman et al., 2001). Finally, cell surface and secreted forms of insulin-degrading enzyme (IDE) have been implicated in Aβ catabolism (Qiu et al., 1998; Vekrellis et al., 2000). Genetic ablation of IDE results in accumulation of unphosphorylated APP fragments without altering phosphorylated fragments, suggesting that IDE activity is localized predominantly near the cell soma (Farris et al., 2003). All three of these enzymes have been shown to influence steady-state levels of Aβ in vivo, and may serve complimentary roles in Aβ catabolism (Iwata et al., 2001; Eckman et al., 2003; Farris et al., 2003; Miller et al., 2003). Thus, altering the subcellular localization of β-cleavage may disrupt the normal catabolic pathways of Aβ, thereby accounting for the different fates of somatic and synaptic Aβ.

In support of the view that the ability of certain Aβ peptides to deposit into amyloid plaques is related to their susceptibility to degradation, Aβ peptides of different lengths were differentially affected by BACE overexpression. The rate-limiting step of Aβ degradation in vivo is the production of Aβ10-37 (Iwata et al., 2000), suggesting that NH_2-terminal truncations may render Aβ peptides more prone to degradation. We found that minimal amounts of the NH_2-terminally

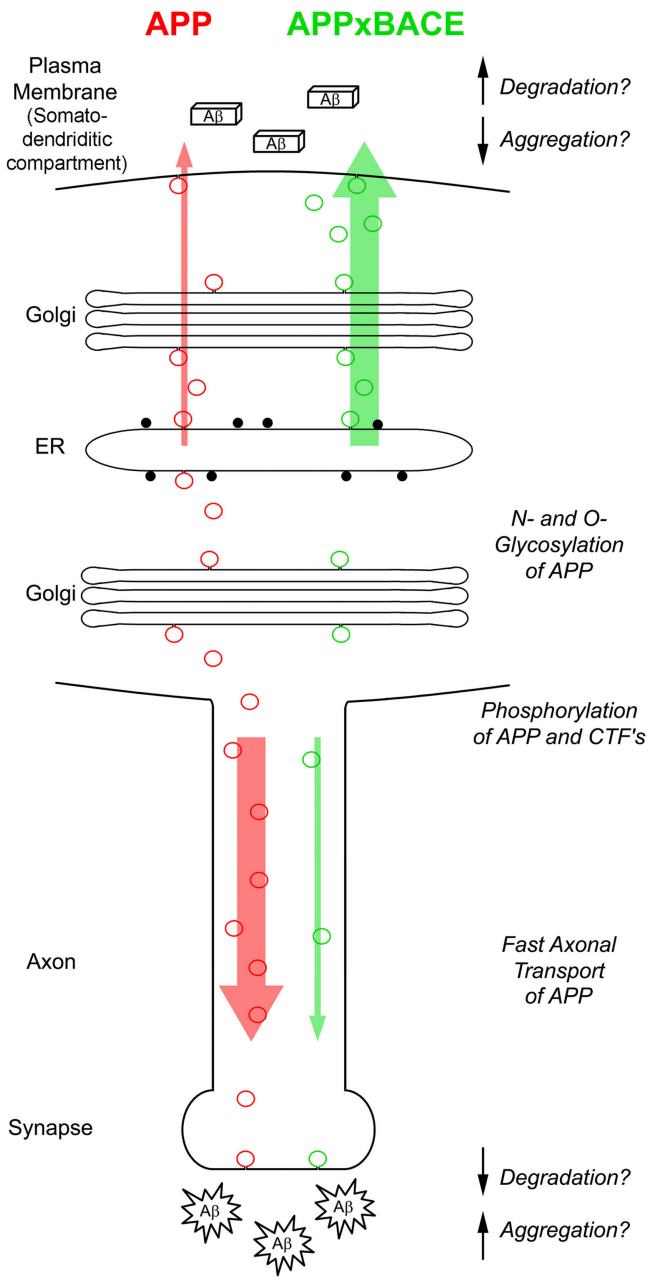

Figure 9. **Subcellular processing of APP and the development of Aβ amyloid pathology.** In monogenic APP mice (red), APP is synthesized in the ER and trafficked to the Golgi apparatus acquiring *N*- and *O*-linked oligosaccharides within these organelles. APP is targeted for fast anterograde axonal transport, coincident with phosphorylation of the COOH terminus of APP. A high proportion of β-cleavage occurs distally within an axonal or synaptic compartment where the likelihood of Aβ degradation diminishes in favor of Aβ secretion and aggregation. BACE overexpression increases β-cleavage such that little APP is targeted to the axon (green) which precludes synaptic targeting and release of Aβ. The inhibition of Aβ pathology due to BACE overexpression indicates that the subcellular localization of Aβ either alters the aggregation kinetics of Aβ, or alters the stability of the peptide due to the intracellular or extracellular localization of Aβ degrading enzymes. Aβ secreted in the somatodendritic compartment (boxes) remains soluble, whereas that released from synaptic terminals (star bursts) deposits into plaques. Red and green circles indicate transported APP in monogenic APP and bigenic APPxBACE mice.

truncated Aβ11-40/42 peptide could be detected upon BACE overexpression despite the increase in C89 levels, supporting the hypothesis that this NH_2-terminal truncated variant is easily degraded in vivo.

In APPxBACE bigenic mice overexpressing the lowest levels of BACE, we observed an increase in Aβ deposition in neocortex, supporting the idea that slight elevations in BACE expression and activity may facilitate the development of AD (Fukumoto et al., 2002; Holsinger et al., 2002). Furthermore, lower levels of BACE overexpression than those reported here increase steady-state Aβ levels in Tg mice (Bodendorf et al., 2002). Nonetheless, the effects of BACE overexpression were not specific to APP harboring the Swedish mutation as BACE overexpression resulted in similar reductions of endogenous and exogenous mature APP in non-Tg mice, APPΔI Tg mice, and human NTera2 cells (Fig. S2, available at http://www.jcb.org/cgi/content/full/jcb.200407070/DC1).

Regardless of the expression level, Aβ deposition was inhibited in the hippocampus. Even at 20 mo old when APPxBACE-M mice accumulate a large amount of brain Aβ deposits, hippocampal Aβ deposits are markedly reduced (Fig. S3, available at http://www.jcb.org/cgi/content/full/jcb.200407070/DC1). We postulate that the region-specific effects of BACE overexpression on Aβ pathology are related to qualitative or quantitative differences in metabolic pathways for APP intrinsic to specific subsets of neurons. For example, mild increases in BACE activity may increase synaptic Aβ in smaller cortical interneurons with relatively short axonal processes. However, due to the length of both the perforant pathway and the mossy fiber pathway, slight elevations in perikaryal BACE activity may preclude synaptic processing of APP in the hippocampus.

Similar region-specific amyloid plaque formation has been observed in the brain of AD patients. For example, whereas association cortices and the limbic system are prone to Aβ amyloid, other regions such as primary sensory/motor neocortices, striatum, brainstem, and spinal cord are relatively unaffected (Braak and Braak, 1991) despite the widespread expression of APP (Tanzi et al., 1987). Interestingly, we found that layer IV neurons within regions of the mouse somatosensory cortex were spared from Aβ pathology in both APP and APPxBACE-M mice (Fig. S3). These layer IV neurons receive a large proportion of their synaptic input from spatially distant thalamic neurons. Although speculative at this point, our results suggest that distinct subsets of neurons and/or the length and number of their efferent inputs may be significant factors that in part determine the regional differences in amyloid pathology found in AD.

In conclusion, although the reduction of Aβ deposition upon BACE overexpression was unexpected, our finding that synaptic Aβ is crucial to the development of amyloid plaques offers several new avenues of research that may improve our understanding of the pathogenesis of amyloid plaques. Thus, further progress toward understanding APP transport, Aβ aggregation within axonal or synaptic vesicles, and the distribution of Aβ degrading enzymes may yield insights which may prove to be clinically relevant.

Materials and methods

Generation of Tg mice

The human BACE cDNA was cloned into the MoPrP.Xho expression vector (Borchelt et al., 1996) at the XhoI restriction site to generate a 15.9-kb NotI linear fragment. DNA was microinjected into C57B6/C3H mouse eggs by the Tg and Chimeric Mouse Facility of the University of Pennsylvania. Genomic DNA was used to identify founders by DNA hybridization of slot blots with ^{32}P-labeled oligonucelotide probes generated from a BACE cDNA PstI digest template. To generate bigenic mice, APP mice (Hsiao et al., 1996) were crossed with BACE Tg lines to generate double heterozygous offspring.

Immunoprecipitation and Western blot analysis

Proteins were extracted by homogenization of tissue in RIPA buffer (0.5% sodium deoxycholate, 0.1% SDS, 1% NP-40, 5 mM EDTA in TBS, pH 8.0) containing protease inhibitors (1 μg/ml of pepstatin A, leupeptin, L-1-tosylamido-2-phenylethyl chloromethyl ketone, 1-chloro-3-tosylamido-7-amino-2-heptanone, soybean trypsin inhibitor, and 0.5 mM PMSF) followed by centrifugation at 100,000 *g* for 20 min at 4°C. When indicated, immunoprecipitations were performed before electrophoresis on either Tris-glycine or 10/16% step-gradient Tris-tricine gels, followed by immunoblotting with the antibodies listed in Table S1, available at http://www.jcb.org/cgi/content/full/jcb.200407070/DC1. For quantification of BACE, serial dilutions of brain lysates were performed to obtain results within the linear range of quantification. For dephosphorylation experiments, COOH-terminal fragments immunoprecipitated with 5685 were treated with *E. coli* alkaline phosphatase at 37°C before electrophoresis.

Sandwich ELISA analysis

Brain regions were sonicated in RIPA buffer (1 ml/150 mg tissue) containing protease inhibitors and centrifuged at 100,000 *g* for 20 min at 4°C. The pellet was sonicated in 70% FA (2 μl/mg tissue) followed by a second of centrifugation. Both RIPA and FA lysates were assayed by sandwich ELISA as previously described (E.B. Lee et al., 2003). Ban50 (anti–$Aβ_{1-10}$) was used to capture full-length Aβ, whereas BC05 and BA27 were used to detect $Aβ_{40}$ and $Aβ_{42}$, respectively. To determine the relative content of NH_2-terminally truncated Aβ, ELISA plates were coated with either JRF/c40 or JRF/c42 to capture $Aβ_{40}$ and $Aβ_{42}$, respectively. The concentrations of full-length Aβ versus total Aβ were determined by using JRF/AβN (anti-$Aβ_{1-7}$) or m266 (anti-$Aβ_{13-28}$) as reporting antibodies.

Histology and immunohistochemistry

Mouse brains were fixed in either ethanol or 4% neutral-buffered formalin for 24 h. Samples were dehydrated through a series of graded ethanol solutions to xylene and infiltrated with paraffin as described previously (Trojanowski et al., 1989). Tissue sections (6 μm) were stained using standard avidin-biotin-peroxidase methods using 3–3′ DAB. BaceN1 (rabbit anti–NH_2 terminus of BACE; Huse et al., 2000), NAB228 (mouse anti-$Aβ_{1-11}$), 4G8 (mouse anti-$Aβ_{17-24}$), m11 (mouse anti-$Aβ_{free11-x}$) and 82 (rabbit anti-$Aβ_{pyro11-x}$) were used as primary antibodies. Thioflavin S staining was used to detect fibrillar Aβ deposits, using Vectashield mounting medium (Vector Laboratories). Images were obtained using 1.25-40×/0.16-0.85 objectives on a microscope (model BX51; Olympus) with a ProgRes C14 Jenoptik camera and software (Laser Optik Systeme). For quantitative image analysis, sections of the somatosensory cortex and hippocampus were stained with NAB228 and analyzed using Image Pro-plus (Media Cybernetics, Inc.).

^{32}P-labeling of phospho-APP

Intravitreal injections of ^{32}P-labeled orthophosphate (250 μCi/2 μl per eye; PerkinElmer) were performed on three pairs of anesthetized APP and APPxBACE-H mice. 6 h after injection, optic nerves were homogenized in RIPA buffer containing protease inhibitors and phosphatase inhibitors (50 mM sodium fluoride and 0.2 mM sodium vanadate), immunoprecipitated with 5685 for full-length APP or RMO26 for NFM (Black and Lee, 1988), separated on a 7.5% Tris-glycine gel, transferred to a nitrocellulose membrane, and exposed to a phosphorimager screen. The same membrane was then immunoblotted with an NH_2-terminal APP antibody (Karen).

Sciatic nerve ligation

Mice were anesthetized and one sciatic nerve from each mouse was ligated approximately in the middle. The other sciatic nerve was used as an unligated control. 6 h after ligation, 5-mm sciatic nerve segments proximal and distal to the ligature were sonicated in RIPA buffer containing protease inhibitors and centrifuged at 100,000 *g* for 20 min at 4°C. Proteins were analyzed by immunoblotting using the antibodies listed in Table S1. Full-length APP, phospho-APP and sAPPβswe were immunoprecipitated with 5685 before immunoblotting.

Spinal cord pulse-labeling

L5 segments of spinal cords from non-Tg and BACE Tg mice were injected with 250 μCi/0.71 μl of [^{35}S]-methionine (PerkinElmer) bilaterally at an infusion rate of 0.1 μl/min. Mice were killed at 0.5, 8, and 16 h after injection when sciatic nerves and spinal cord segments 2-mm rostral and caudal to the injection site were harvested. Samples were homogenized with RIPA buffer, immunoprecipitated with 5685 for full-length APP, and electrophoresed on 7.5% Tris-glycine gels. Radiolabeled APP was quantified by ImageQuant phosphorimager analysis (Molecular Dynamics).

Online supplemental material

Table S1 lists the antibodies used for biochemical analysis. Fig. S1 shows immunohistochemical and biochemical analysis of full-length and truncated Aβ in aged Tg mice. Fig. S2 shows the reduction of mature APP in APPΔI Tg mice and human neuronal cultures upon BACE overexpression. Fig. S3 shows the regional distribution of amyloid pathology in 20-mo-old Tg mice. Online supplemental material is available at http://www.jcb.org/cgi/content/full/jcb.200407070/DC1.

We gratefully thank Takeda Pharmaceutical, Janssen Pharmaceutical, and Eli Lilly for providing monoclonal antibodies for the Aβ sandwich ELISAs and immunohistochemistry. The authors would like to thank S. Leight, K. Lindeen, D. Martinez, T. Schuck, and I. Solano for technical advice and assistance, and Dr. A. Crystal, Dr. J. Huse, L. Kim, V. Morais, and Dr. C. Wilson for valuable discussions.

This work was supported in part by National Institutes of Health training grant T32 AG00255 (to E.B. Lee) and NIA AG11542. R.W. Doms was also supported by a Paul Beeson Faculty Scholar Award, J.Q. Trojanowski is the Measey-Schnabel Professor of Geriatric Medicine and Gerontology and V.M.-Y. Lee is the John H. Ware III Professor of Alzheimer's research.

Submitted: 12 July 2004
Accepted: 22 November 2004

References

Ando, K., M. Oishi, S. Takeda, K. Iijima, T. Isohara, A.C. Nairn, Y. Kirino, P. Greengard, and T. Suzuki. 1999. Role of phosphorylation of Alzheimer's amyloid precursor protein during neuronal differentitation. *J. Neurosci.* 19:4421–4427.

Black, M.M., and V.M.-Y. Lee. 1988. Phosphorylation of neurofilament proteins in intact neurons: demonstration of phosphorylation in cell bodies and axons. *J. Neurosci.* 8:3296–3305.

Bodendorf, U., S. Danner, F. Fischer, M. Stefani, C. Sturchler-Pierrat, K.H. Wiederhold, M. Staufenbiel, and P. Paganetti. 2002. Expression of human β-secretase in the mouse brain increases the steady-state level of β-amyloid. *J. Neurochem.* 80:799–806.

Borchelt, D.R., J. Davis, M. Fischer, M.K. Lee, H.H. Slunt, T. Ratovitsky, J. Regard, N.G. Copeland, N.A. Jenkins, S.S. Sisodia, and D.L. Price. 1996. A vector for expressing foreign genes in the brains and hearts of Tg mice. *Genet. Anal.* 13:159–163.

Borchelt, D.R., T. Ratovitski, J. van Lare, M.K. Lee, V. Gonzales, N.A. Jenkins, N.G. Copeland, D.L. Price, and S.S. Sisodia. 1997. Accelerated amyloid deposition in the brains of Tg mice coexpressing mutant presenilin 1 and amyloid precursor proteins. *Neuron.* 19:939–945.

Braak, H., and E. Braak. 1991. Neuropathological stageing of Alzheimer-related changes. *Acta Neuropathol. (Berl.).* 82:239–259.

Buxbaum, J.D., G. Thinakaran, V. Koliatsos, J. O'Callahan, H.H. Slunt, D.L. Price, and S.S. Sisodia. 1998. Alzheimer amyloid protein precursor in the rat hippocampus: transport and processing through the perforant path. *J. Neurosci.* 18:9629–9637.

Cai, H., Y. Wang, D. McCarthy, H. Wen, D.R. Borchelt, D.L. Price, and P.C. Wong. 2001. BACE1 is the major β-secretase for generation of Aβ peptides by neurons. *Nat. Neurosci.* 4:233–234.

Eckman, E.A., D.K. Reed, and C.B. Eckman. 2001. Degradation of the Alzheimer's amyloid β peptide by endothelin-converting enzyme. *J. Biol. Chem.* 276:24540–24548.

Eckman, E.A., M. Watson, L. Marlow, K. Sambamurti, and C.B. Eckman. 2003. Alzheimer's disease β-amyloid peptide is increased in mice deficient in endothelin-converting enzyme. *J. Biol. Chem.* 278:2081–2084.

Farris, W., S. Mansourian, Y. Chang, L. Lindsley, E.A. Eckman, M.P. Frosch, C.B. Eckman, R.E. Tanzi, D.J. Selkoe, and S. Guenette. 2003. Insulin-degrading enzyme regulates the levels of insulin, amyloid β-protein, and

the β-amyloid precursor protein intracellular domain in vivo. *Proc. Natl. Acad. Sci. USA.* 100:4162–4167.

Ferreira, A., A. Caceres, and K.S. Kosik. 1993. Intraneuronal compartments of the amyloid precursor protein. *J. Neurosci.* 13:3112–3123.

Follet, J., C. Lemaire-Vieille, F. Blanquet-Grossard, V. Podevin-Dimster, S. Lehmann, J.P. Chauvin, J.P. Decavel, R. Varea, J. Grassi, M. Fontes, and J.Y. Cesbron. 2002. PrP expression and replication by Schwann cells: implications in prion spreading. *J. Virol.* 76:2434–2439.

Fukami, S., K. Watanabe, N. Iwata, J. Haraoka, B. Lu, N.P. Gerard, C. Gerard, P. Fraser, D. Westaway, P. George-Hyslop, and T.C. Saido. 2002. Aβ-degrading endopeptidase, neprilysin, in mouse brain: synaptic and axonal localization inversely correlating with Aβ pathology. *Neurosci. Res.* 43:39–56.

Fukumoto, H., B.S. Cheung, B.T. Hyman, and M.C. Irizarry. 2002. β-Secretase protein and activity are increased in the neocortex in Alzheimer disease. *Arch. Neurol.* 59:1381–1389.

Games, D., D. Adams, R. Alessandrini, R. Barbour, P. Berthelette, C. Blackwell, T. Carr, J. Clemens, T. Donaldson, F. Gillespie, et al. 1995. Alzheimer-type neuropathology in Tg mice overexpressing V717F β-amyloid precursor protein. *Nature.* 373:523–527.

Gouras, G.K., H. Xu, J.N. Jovanovic, J.D. Buxbaum, R. Wang, P. Greengard, N.R. Relkin, and S. Gandy. 1998. Generation and regulation of β-amyloid peptide variants by neurons. *J. Neurochem.* 71:1920–1925.

Holsinger, R.M., C.A. McLean, K. Beyreuther, C.L. Masters, and G. Evin. 2002. Increased expression of the amyloid precursor β-secretase in Alzheimer's disease. *Ann. Neurol.* 51:783–786.

Hsiao, K., P. Chapman, S. Nilsen, C. Eckman, Y. Harigaya, S. Younkin, F. Yang, and G. Cole. 1996. Correlative memory deficits, Aβ elevation, and amyloid plaques in Tg mice. *Science.* 274:99–102.

Huse, J.T., D.S. Pijak, G.J. Leslie, V.M.-Y. Lee, and R.W. Doms. 2000. Maturation and endosomal targeting of β-site amyloid precursor protein-cleaving enzyme. The Alzheimer's disease β-secretase. *J. Biol. Chem.* 275:33729–33737.

Huse, J.T., K. Liu, D.S. Pijak, D. Carlin, V.M.-Y. Lee, and R.W. Doms. 2002. β-Secretase processing in the trans-Golgi network preferentially generates truncated amyloid species that accumulate in Alzheimer's disease brain. *J. Biol. Chem.* 277:16278–16284.

Iijima, K., K. Ando, S. Takeda, Y. Satoh, T. Seki, S. Itohara, P. Greengard, Y. Kirino, A.C. Nairn, and T. Suzuki. 2000. Neuron-specific phosphorylation of Alzheimer's β-amyloid precursor protein by cyclin-dependent kinase 5. *J. Neurochem.* 75:1085–1091.

Iwata, N., S. Tsubuki, Y. Takaki, K. Watanabe, M. Sekiguchi, E. Hosoki, M. Kawashima-Morishima, H.J. Lee, E. Hama, Y. Sekine-Aizawa, and T.C. Saido. 2000. Identification of the major Aβ1-42-degrading catabolic pathway in brain parenchyma: suppression leads to biochemical and pathological deposition. *Nat. Med.* 6:143–150.

Iwata, N., S. Tsubuki, Y. Takaki, K. Shirotani, B. Lu, N.P. Gerard, C. Gerard, E. Hama, H.J. Lee, and T.C. Saido. 2001. Metabolic regulation of brain Aβ by neprilysin. *Science.* 292:1550–1552.

Kamenetz, F., T. Tomita, H. Hsieh, G. Seabrook, D. Borchelt, T. Iwatsubo, S. Sisodia, and R. Malinow. 2003. APP processing and synaptic function. *Neuron.* 37:925–937.

Koo, E.H., S.S. Sisodia, D.R. Archer, L.J. Martin, A. Weidemann, K. Beyreuther, P. Fischer, C.L. Masters, and D.L. Price. 1990. Precursor of amyloid protein in Alzheimer disease undergoes fast anterograde axonal transport. *Proc. Natl. Acad. Sci. USA.* 87:1561–1565.

Lazarov, O., M. Lee, D.A. Peterson, and S.S. Sisodia. 2002. Evidence that synaptically released β-amyloid accumulates as extracellular deposits in the hippocampus of Tg mice. *J. Neurosci.* 22:9785–9793.

Lee, E.B., D.M. Skovronsky, F. Abtahian, R.W. Doms, and V.M.-Y. Lee. 2003. Secretion and intracellular generation of truncated Aβ in β-site amyloid-β precursor protein-cleaving enzyme expressing human neurons. *J. Biol. Chem.* 278:4458–4466.

Lee, J.Y., T.B. Cole, R.D. Palmiter, S.W. Suh, and J.Y. Koh. 2002. Contribution by synaptic zinc to the gender-disparate plaque formation in human Swedish mutant APP Tg mice. *Proc. Natl. Acad. Sci. USA.* 99:7705–7710.

Lee, M.S., S.C. Kao, C.A. Lemere, W. Xia, H.C. Tseng, Y. Zhou, R. Neve, M.K. Ahlijanian, and L.H. Tsai. 2003. APP processing is regulated by cytoplasmic phosphorylation. *J. Cell Biol.* 163:83–95.

Lin, X., G. Koelsch, S. Wu, D. Downs, A. Dashti, and J. Tang. 2000. Human aspartic protease memapsin 2 cleaves the β-secretase site of β-amyloid precursor protein. *Proc. Natl. Acad. Sci. USA.* 97:1456–1460.

Liu, K., R.W. Doms, and V.M.-Y. Lee. 2002. Glu11 site cleavage and N-terminally truncated Aβ production upon BACE overexpression. *Biochemistry.* 41:3128–3136.

Luo, Y., B. Bolon, S. Kahn, B.D. Bennett, S. Babu-Khan, P. Denis, W. Fan, H. Kha, J. Zhang, Y. Gong, et al. 2001. Mice deficient in BACE1, the Alzheimer's β-secretase, have normal phenotype and abolished β-amyloid generation. *Nat. Neurosci.* 4:231–232.

Miller, B.C., E.A. Eckman, K. Sambamurti, N. Dobbs, K.M. Chow, C.B. Eckman, L.B. Hersh, and D.L. Thiele. 2003. Amyloid-β peptide levels in brain are inversely correlated with insulysin activity levels in vivo. *Proc. Natl. Acad. Sci. USA.* 100:6221–6226.

Qiu, W.Q., D.M. Walsh, Z. Ye, K. Vekrellis, J. Zhang, M.B. Podlisny, M.R. Rosner, A. Safavi, L.B. Hersh, and D.J. Selkoe. 1998. Insulin-degrading enzyme regulates extracellular levels of amyloid β-protein by degradation. *J. Biol. Chem.* 273:32730–32738.

Schubert, W., R. Prior, A. Weidemann, H. Dircksen, G. Multhaup, C.L. Masters, and K. Beyreuther. 1991. Localization of Alzheimer βA4 amyloid precursor protein at central and peripheral synaptic sites. *Brain Res.* 563:184–194.

Schweizer, A., O. Valdenaire, P. Nelbock, U. Deuschle, J.B. Dumas Milne Edwards, J.G. Stumpf, and B.M. Loffler. 1997. Human endothelin-converting enzyme (ECE-1): three isoforms with distinct subcellular localizations. *Biochem. J.* 328:871–877.

Sheng, J.G., D.L. Price, and V.E. Koliatsos. 2002. Disruption of corticocortical connections ameliorates amyloid burden in terminal fields in a Tg model of Aβ amyloidosis. *J. Neurosci.* 22:9794–9799.

Sinha, S., J.P. Anderson, R. Barbour, G.S. Basi, R. Caccavello, D. Davis, M. Doan, H.F. Dovey, N. Frigon, J. Hong, et al. 1999. Purification and cloning of amyloid precursor protein β-secretase from human brain. *Nature.* 402:537–540.

Skovronsky, D.M., D.B. Moore, M.E. Milla, R.W. Doms, and V.M.-Y. Lee. 2000. Protein kinase C-dependent α-secretase competes with β-secretase for cleavage of amyloid-β precursor protein in the trans-Golgi network. *J. Biol. Chem.* 275:2568–2575.

Tanzi, R.E., J.F. Gusella, P.C. Watkins, G.A. Bruns, P. George-Hyslop, M.L. Van Keuren, D. Patterson, S. Pagan, D.M. Kurnit, and R.L. Neve. 1987. Amyloid β protein gene: cDNA, mRNA distribution, and genetic linkage near the Alzheimer locus. *Science.* 235:880–884.

Trojanowski, J.Q., T. Schuck, M.L. Schmidt, and V.M.-Y. Lee. 1989. Distribution of tau proteins in the normal human central and peripheral nervous system. *J. Histochem. Cytochem.* 37:209–215.

Vassar, R., B.D. Bennett, S. Babu-Khan, S. Kahn, E.A. Mendiaz, P. Denis, D.B. Teplow, S. Ross, P. Amarante, R. Loeloff, et al. 1999. β-Secretase cleavage of Alzheimer's amyloid precursor protein by the transmembrane aspartic protease BACE. *Science.* 286:735–741.

Vekrellis, K., Z. Ye, W.Q. Qiu, D. Walsh, D. Hartley, V. Chesneau, M.R. Rosner, and D.J. Selkoe. 2000. Neurons regulate extracellular levels of amyloid β-protein via proteolysis by insulin-degrading enzyme. *J. Neurosci.* 20:1657–1665.

Wang, R., D. Sweeney, S.E. Gandy, and S.S. Sisodia. 1996. The profile of soluble amyloid β protein in cultured cell media. Detection and quantification of amyloid β protein and variants by immunoprecipitation-mass spectrometry. *J. Biol. Chem.* 271:31894–31902.

Wilson, C.A., R.W. Doms, and V.M.-Y. Lee. 1999. Intracellular APP processing and Aβ production in Alzheimer disease. *J. Neuropathol. Exp. Neurol.* 58:787–794.

Yan, R., M.J. Bienkowski, M.E. Shuck, H. Miao, M.C. Tory, A.M. Pauley, J.R. Brashier, N.C. Stratman, W.R. Mathews, A.E. Buhl, et al. 1999. Membrane-anchored aspartyl protease with Alzheimer's disease β-secretase activity. *Nature.* 402:533–537.